A DIRECT DETERMINATION OF $\alpha_S(Q^2)$ AND $f_{g/p}(\xi, Q^2)$ IN NEXT-TO-LEADING-ORDER FROM (2+1)-JET RATES IN THE H1-EXPERIMENT[a]

K. ROSENBAUER

I. Physikalisches Institut RWTH Aachen

Sommerfeldstraße, D-52056 Aachen, Germany

On behalf of the H1 collaboration

Firstly, the analysis method of the determination of the running strong coupling constant $\alpha_S(Q^2)$ based on jet rates in deep inelastic ep-scattering at HERA will be briefly reviewed. In this context, the effects on the measured value $\alpha_S(M_Z^2)$ of different recombination schemes while defining the jet multiplicity for an event with the JADE algorithm is studied. Secondly, a next-to-leading-order extraction of the gluon density in the proton as well from jet rates by using the technique of Mellin transforms will be discussed and preliminary results are presented.

1 Introduction

The physics of jets in deeply inelastic scattering is a promising subject at HERA. The production rate of multi-jet events is a function of both the strong coupling constant $\alpha_S(\mu_r^2)$ and the gluon density $f_{g/p}(\xi, \mu_f^2)$ in the proton.[b] μ_r, μ_f abbreviate the renormalization and factorization scale and ξ denotes the fractional momentum of the incoming parton to the hard subprocess with respect to the momentum of the parent particle, the proton. With the limited statistic given by the data taken in 1994 with the H1 detector corresponding to an integrated luminosity of $\mathcal{L} = 2.74\,\mathrm{pb}^{-1}$, it is not possible to determine both quantities simultaneously. In the following, separate determinations of $\alpha_S(\mu_r^2)$ and $f_{g/p}(\xi, \mu_f^2)$ in next-to-leading-order (NLO) using fractional (2+1)-jet rates are presented.

1.1 QCD corrections

In lowest order, the electron scatters off a quark via a single photon exchange[c] leading to a (1+1)-jet event. One jet is caused by the scattered quark, the other by the remaining part of the proton (+1), which is only partially observed in the detector. Higher jet multiplicities are described in the framework of QCD.

[a] Talk presented at the Workshop on DIS and Related Phenomena, Roma, April 1996.

[b] Of course the cross section depends on the well known quark densities as well.

[c] The exchange of the intermediate Z^0 boson is highly suppressed due to it's large mass.

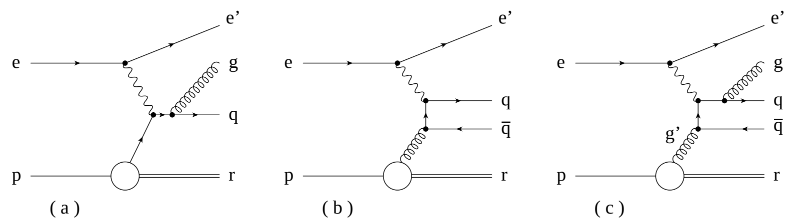

Figure 1: Generic Feynman diagrams for the LO processes of QCD Compton scattering QCDC (a) and photon-gluon fusion BGF (b), and an example of a diagram corresponding to a NLO real correction (c).

The NLO cross section for the (2+1)-jet final state can be written formally in the form

$$\begin{aligned}\sigma_{2+1}^{NLO} \;=\; & \textstyle\sum_{i=q,g} \int \mathrm{d}\xi \;\; f_{i/p}(\xi,\mu_f^2) \times \{\alpha_S(\mu_r^2) A_{\text{Born}}^{(i)}(\xi) \\ & + \alpha_S(\mu_r^2)^2 \left[A_{\text{virt.}}^{(i)}(\xi,\mu_r^2) + A_{\text{real}}^{(i)}(\xi,\mu_f^2)\right]\}. \end{aligned} \tag{1}$$

In lowest order (1+1)-jet events ξ equals the Bjorken x variable, whereas in (2+1)-jet events, see QCDC and BGF in fig. 1, ξ is given by:

$$\xi = x\left(1 + \frac{\hat{s}}{Q^2}\right). \tag{2}$$

$\hat{s}$ denotes the invariant mass squared of the hard subprocess and Q^2 the negative four momentum transfer squared between the in- and outgoing electron. Diagrams of the type shown in fig. 1c can also lead to (2+1)-jet configurations. Then, in certain kinematical regions, ξ is no longer an observable and the distinction between QCDC and BGF becomes meaningless. Therefore the gluon density can only be determined in NLO via a fit.

In the studies presented here, μ_r^2 and μ_f^2 are identified with Q^2. At large Q^2 the (2+1)-jet cross section is dominated by quark initiated processes and the corresponding parton densities are well known. Hence the Q^2 range $150 < Q^2 < 4000$ GeV^2 is used for the determination of $\alpha_S(Q^2)$. For the extraction of $f_{g/p}(\xi, Q^2)$ the Q^2 range is extended down to 40 GeV^2 because at small values of Q^2 small ξ values are accessible and in this region the BGF becomes dominating.[d] The chosen lower cut-off in Q^2 suppresses events with the emission of multi-gluon radiation from the initial state partons, which is naturally not taken into account by a fixed order theory. Besides, this cut-off ensures that the NLO corrections are reasonably small and the perturbative QCD can be considered as an applicable theory.

[d]It has been pointed out[1] that $f_{g/p}(\xi, Q^2)$ is not yet well constrained for $0.01 < \xi < 0.1$.

1.2 JADE algorithm and recombination schemes

In the last few years the only available (2+1)-jet cross section NLO calculations were based on a modified JADE algorithm as implemented in PROJET[2] and DISJET.[3] The resolution criterion is $y_{ij} = 2E_iE_j(1-\cos\theta_{ij})/W^2 > y_c$, where y_c is the resolution parameter. W^2 denotes the invariant mass squared of the total hadronic energy including a pseudo-particle, which represents the missing longitudinal momentum of the event, since the proton remnant is included in the jet definition. With the value $y_c = 0.02$ chosen the (2+1)-jet events probe the parton density functions at $\xi > y_c = 0.02$ (see eq. 2).

While in the experiment one has to distinguish between different recombination schemes (RS) if two objects i and j have to be recombined to a new one k the procedure used in PROJET can not be identified with one of these RS. In the so called Jade RS the four-momentum-vector p_k is simply given by $p_k = p_i + p_j$, whereas in the E0 RS ($p_k = (E_i + E_j, (E_i + E_j) * \frac{\vec{p}_i+\vec{p}_j}{|\vec{p}_i+\vec{p}_j|})$) and P RS ($p_k = (|\vec{p}_i + \vec{p}_j|, \vec{p}_i + \vec{p}_j)$), the new vector should be massless. In PROJET the resulting four-vectors are massless, too. With the availability of the new σ-Monte-Carlo MEPJET, the (2+1)-jet cross section is calculable for all three RS.[4] As long as there are no cuts applied on energy or momentum of the final jets, the Jade and E0 RS are equivalent in the theoretical NLO calculations. In the experiment the results of Jade and E0 agree at a level of a few percent, whereas the (2+1)-jet cross section using the P RS is lowered by up to 20%.

2 The determination of the strong coupling

The analysis presented here essentially follows the strategy of the previous measurement.[5] The fractional (2+1)-jet rate $R_{2+1}(Q^2, y_c) = \frac{\sigma_{2+1}(Q^2,y_c)}{\sigma_{\rm tot}(Q^2)} = f(\alpha_S(Q^2))$ is chosen[6] to explore the running of $\alpha_S(Q^2)$. Theoretically, R_{2+1} is known to NLO, i.e. up to $\mathcal{O}(\alpha_S^2)$.[2,4] Experimentally, R_{2+1} is obtained by N_{2+1}/N_{tot} where N_{2+1} is the number of events with 2 observed current jets in the final acceptance region and N_{tot} the number of events with one or two jets in this region. Using a full event generator like LEPTO 6.3[7], these measured jet rates at the detector level are corrected to the parton level, where they can be compared with the NLO QCD-prediction. The independent measurements in bins of Q^2 are then used to determine $\alpha_S(M_Z^2)$ by performing a fit to the renormalization group equation (RGE) as already discussed previously.[5]

The use of PROJET as in earlier analyses[5,8] in combination with the Jade RS on the experimental side results in $\alpha_S(M_Z^2) = 0.124 \pm 0.006(\text{stat.}) \pm 0.008(\text{sys.})$, which in view of the theoretical difficulties described above should not be taken too seriously. This value relies on the event selection requirements:

Table 1: Values of $\alpha_S(M_Z^2)$ extracted with PROJET and MEPJET applying different recombination schemes (RS) in the JADE algorithm and using the MRSH parton density parametrization.[9] The statistical errors are of the order 5%.

RS	Jade	E0	P
PROJET	0.124	0.127	0.114
MEPJET	0.110	0.112	0.112

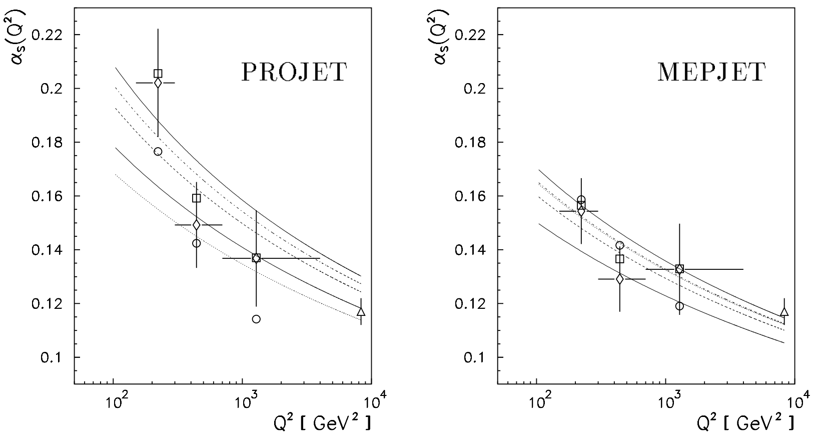

Figure 2: The derived α_S values ($\diamond$, $\square$, $\circ$) together with the fit results (dashed, dashed-dotted and dotted lines) for the three different RS Jade, E0 and P used in the JADE algorithm. For the Jade scheme the one σ parameter errors (solid lines) are also plotted. Only the statistical errors from the data and the correction factors are shown. The open triangle $\triangle$ at $Q^2 = M_Z^2$ indicates the world average $\alpha_S(M_Z^2) = 0.117 \pm 0.005$.

$W^2 > 5000$ GeV^2, $E_e > 11$ GeV, $10° < \theta_e < 150°$, and $y_e < 0.7$. To suppress higher order QCD-effects jet acceptance cuts are applied: $10° < \theta_{jet} < 145°$ and for $(2+1)$-jet events in addition $z_p > 0.1$. In the CMS of the hard subprocess z_p is defined by the smaller $(\theta^\star_{jet})$ of the jet angles (with respect to the incoming parton) of the two jets: $z_p = \frac{1}{2}(1 - \cos\theta^\star_{jet})$. The systematic error was estimated by analyzing different scenarios taking into account possible correlations between the error sources. The error includes uncertainties due to detector effects, acceptance cuts, QCD models, hadronization effects, parton densities (and the used Λ_{QCD} therein), y_c, μ_r, and μ_f.

Whereas the resulting $\alpha_S(M_Z^2)$ value depends strongly on the RS applied by using PROJET for the NLO calculation, the result seems to be independent of the RS for MEPJET (see table 1). The values $\alpha_S(M_Z^2)$ and $\alpha_S(Q^2)$ in the different Q^2 bins (fig. 2) reflect that the (2+1)-jet cross sections from PROJET in the different Q^2 bins are close to the calculated ones from MEPJET using the P RS. But the discrepancy increases with decreasing Q^2. The shape of the $\alpha_S(Q^2)$ values extracted by using PROJET seems to be steeper than the prediction of the RGE. In contrast to that, the "MEPJET $\alpha_S(Q^2)$ values" follow nicely the RGE prediction for all three RS and they are close together for the different RS. One reason for the differences between the results of PROJET and MEPJET may be that in PROJET terms proportional to $y_c \cdot W^2$ are neglected. In combination with the relation $W^2 = ys - Q^2$, deviations are expected in the low Q^2 region.

3 The determination of the gluon density

The only way to achieve a direct NLO determination of $f_{g/p}(\xi, Q^2)$ is to parametrize the function $f_{g/p}$ at a given scale Q_0^2, to evolve it then to a value of Q^2 where the cross section is measured and to fit the parameters of $f_{g/p}$ with respect to suitably infrared safe observable. The expression

$$f_{g/p}(\xi, Q_0^2) = A_N \xi^{\alpha} (1-\xi)^{\beta} (1+\gamma\xi) \tag{3}$$

is used as parametrization ansatz with three free parameters (α, β, γ) and the MRSD-$'$ quark parametrization[10] at the scale $Q_0^2 = 4$ GeV^2 as input. The uncertainty of the quark density can be neglected in the considered kinematical range. As observable the (2+1)-jet rate $R_{2+1}(Q^2)$ (corrected to parton level) is used in four bins of Q^2 between 40 and 4000 GeV^2. For $Q^2 > 100$ GeV^2, the analysis is based on the same event selection as the α_S measurement with an additional cut $\theta_q < 100°$. θ_q is calculated from the electron variables alone and corresponds to the angle of the recoiling quark in the quark parton model. The kinematical selection criteria for $Q^2 < 100$ GeV^2 are: $W^2 > 5000$ GeV^2, $E_e > 14$ GeV, $160° < \theta_e < 173°$, and $\theta_q < 100°$. To suppress higher order QCD-effects, the same jet acceptance cuts are applied as discussed above.

In fitting the free parameters of $f_{g/p}$ a severe practical problem is that the cross section (respectively the rate R_{2+1}) has to be evaluated repeatedly for every choice of parameters for $f_{g/p}$. The DGLAP evolution of the gluon density in the x-space and the subsequent Monte-Carlo integration takes too much CPU-time. Therefore the technique of Mellin transforms is used for a fast numerical evaluation of the cross section.[11] The moments in the Mellin space are defined by $f_n \equiv \int_0^1 \frac{\mathrm{d}x}{x} x^n f(x)$ for an arbitrary function f and (complex) n. It can be demonstrated[11] that the moments $\tilde{\Sigma}_{na}$ of the gluon initiated cross section Σ_a (integrated over an x-range from a to 1) are given by: $\tilde{\Sigma}_{na} =$

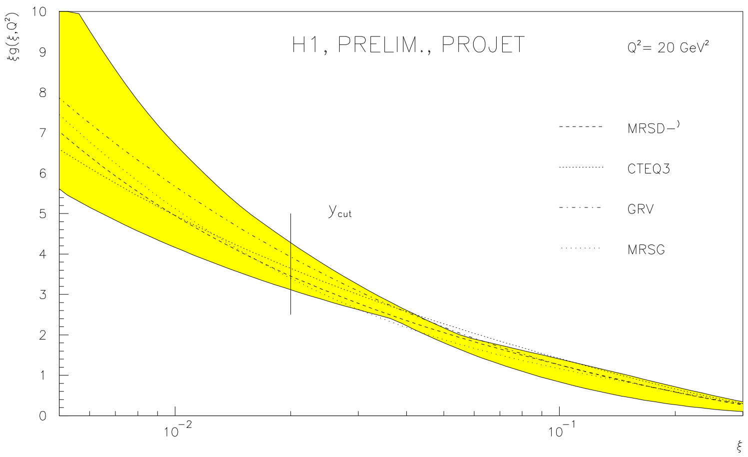

Figure 3: The gluon density in NLO by H1 (prel.) compared to other parametrizations like MRSD-',[10] CTEQ3,[13] GRV,[14] and MRSG.[15] The shaded area represents the obtained range for $f_{g/p}$ using the JADE algorithm in combination with the Jade RS.

$f_{g/p,n}(Q^2) \cdot h_{an}$. $f_{g/p,n}$ denotes the moments of the gluon density. The h_{an} are the Σ_a with the parton density replaced by $(a/\xi)^n$ and hence they correspond, in some way, to the moments of the cross section of the hard subprocess. The cross section Σ_a in the x-space can be determined from the moments $\tilde{\Sigma}_{na}$ by an inverse Mellin transform. The only time-consuming step of calculating the moments h_{an} — currently possible only with PROJET — has to be done in the fit only once.

The parameter β in the ansatz for the gluon density gets more important for "high" ξ and is therefore not strongly constrained by the present data at HERA. This uncertainty is fixed by introducing an additional point at $\xi = 0.2$ taking into account the world error.[12] The systematic errors of $R_{2+1}(Q^2)$ are treated similarly to the error determination in the α_S-measurements. The error on the gluon density is estimated by varying the parameters within the $\pm 1\sigma$-errors and taking the maximum spread. Fig. 3 shows the extracted gluon density in NLO using the Jade RS. In the ξ-range where the fit is performed ($\xi > y_c$), other frequently used parametrizations lie within the fitted range.

Acknowledgments

It is a pleasure to thank the H1 collab., in particular M. Hampel, Ch. Niedzballa, and K. Rabbertz, for communicating and discussing their results.

References

1. W.J. Stirling, Structure Functions, talk given at Workshop on Deep Inelastic Scattering and QCD (DIS 95), Paris, France, 24-28 Apr. 1995.
2. D. Graudenz, PROJET4.1, CERN-TH.7420/94.
3. T. Brodkorb and E. Mirkes, DISJET manual, Univ. of Wisconsin, MAD/PH/821 (1994);
   T. Brodkorb and E. Mirkes, Univ. of Wisconsin, MAD/PH/820 (1994).
4. E. Mirkes and D. Zeppenfeld, MADPH-95-916.
5. H1 Collaboration, T. Ahmed et al., Phys. Lett. **B346** (1995) 415.
6. R. Nisius, PhD thesis, Aachen preprint PITHA 94/21 (1994).
7. G. Ingelman, LEPTO version 6.3, unpublished program manual; see also: LEPTO 6.1, Proc. Workshop ‘Physics at HERA’, DESY, Hamburg, Vol. 3 (1991) 1366.
8. H1 Collaboration, "Determination of the Strong Coupling Constant α_S in Deep Inelastic *ep* Scattering at HERA", paper EPS-0485 submitted to the 1995 Europhysics Conference, Brussels, Belgium.
9. A.D. Martin, W.J. Stirling and R.G. Roberts, Proc. of the Workshop on Quantum Field theory and Theoretical Aspects of High Energy Physics, eds. B. Geyer and E.M. Ilgenfritz, 11 (1993), Durham, DTP 93-86, and Rutherford, RAL 93-077.
10. A.D. Martin, W.J. Stirling and R.G. Roberts, Phys. Lett. **B306** (1993) 145.
11. D. Graudenz, M. Hampel, A. Vogt and Ch. Berger, Z. Phys. **C70** (1996) 770.
12. W. Vogelsang and A. Vogt, preprint DESY 95-096 (1995).
13. CTEQ Collaboration, H.L. Lai et al., Phys. Rev. **D51** (1995) 4763.
14. M. Glück, E. Reya and A. Vogt, Z. Phys. **C67** (1995) 433-448.
15. A.D. Martin, W.J. Stirling and R.G. Roberts, RAL preprint RAL-95-021.